# Comparing plasmonic electrodes prepared by electron-beam lithography and electrochemical reduction of an Au (iii) salt: application in active plasmonic devices

To cite this article: Van-Quynh Nguyen *et al* 2016 *Adv. Nat. Sci: Nanosci. Nanotechnol.* **7** 015005

View the article online for updates and enhancements.

You may also like

- Surface plasmon resonance in gold nanoparticles: a review
  Vincenzo Amendola, Roberto Pilot, Marco Frasconi et al.

- Fabrication of aluminium nanostructures for plasmonics
  Jérôme Martin and Jérôme Plain

- Ag–Cu mixed phase plasmonic nanostructures fabricated by shadow nanosphere lithography and glancing angle co-deposition
  Whitney Ingram, Steven Larson, Daniel Carlson et al.

# Comparing plasmonic electrodes prepared by electron-beam lithography and electrochemical reduction of an Au(III) salt: application in active plasmonic devices

**Van-Quynh Nguyen**[1,2]**, Delphine Schaming**[1]**, Pascal Martin**[1] **and Jean-Christophe Lacroix**[1]

[1] Université Paris Diderot, Sorbonne Paris Cité, ITODYS, UMR 7086 CNRS, 15 rue Jean-Antoine de Baïf, F-75205 Paris Cedex 13, France
[2] University of Science and Technology of Hanoi (USTH), 18 Hoang Quoc Viet, Hanoi, Vietnam

E-mail: lacroix@univ-paris-diderot.fr

### Abstract
This work describes two different methods for obtaining electrodes covered with gold nanoparticles: electron-beam lithography and electroreduction of an Au(III) salt by chronoamperometry. Localized surface plasmon resonances of these different electrodes have been compared. In a second step, these plasmonic AuNP electrodes were covered with an ultrathin organic film of bisthienylbenzene which displays a reversible voltage-dependent switch between conducting and insulating states. The effect of this conductance switch on the plasmonic properties of the AuNPs has been studied.

## 1. Introduction

Noble metal (gold or silver for instance) nanoparticles (NPs) have been particularly investigated these last decades, due to their remarkable optical and chemical properties. Indeed, they have applications in many fields, such as optics, electronics, photoelectric devices, catalysis, medicine, sensors… For some of these applications, it is necessary to immobilize the NPs on solid substrates. Several methods for immobilizing NPs on substrates have been reported. While it is possible to adsorb colloidal NPs by electrostatic interaction [1] or by using binding molecules [2], it is also possible to obtain NPs directly on the surface. In particular, a classical method for fabricating substrates with NPs of regular size and controlled

shape is electron-beam (*e*-beam) lithography [3–7]. Another classical method relies on vapor-phase gold deposition through a template using polystyrene nanospheres [8–10]. While well-ordered NP arrays can be obtained by these techniques, an easier and cheaper method of making AuNP substrates is the electrochemical reduction of a metal salt, even if this method leads to non-ordered substrates [11, 12].

An interesting property of such AuNPs is their localized surface plasmon resonance (LSPR). This phenomenon corresponds to collective oscillations of the free electrons of NPs, leading at a particular frequency to a resonance phenomenon. This results in a strong optical extinction in the visible or the near-infrared spectral regions. The optical behavior, defined by the resonance wavelength, the bandwidth and the amplitude of the LSPR, depends on the metal of the NPs, their size, their shape, and the dielectric constant of the surrounding medium. Active plasmonic devices, i.e. plasmonic systems for which an external stimulus can reversibly tune the wavelength and/or the amplitude of the LSPR, are the subject

of important research efforts. The easiest way to obtain such active plasmonic devices consists in surrounding NPs with switchable materials whose effective dielectric constant is changed by an external input. Several external stimuli have already been employed, based on thermo- [13–15], pH- [16], photo- [17, 18], electrical- [19] and redox-responsive [3–7, 20–24] materials, these stimuli allowing to change the phase [13, 14, 17–19], the spin [15] or the conductivity [3–7, 21, 23, 24] of the material. In particular, electrochemically driven active plasmonic devices have been studied by using conducting polymers as the surrounding media: polyaniline (PANI) [3–5, 21, 23], poly(3,4-ethylenedioxythiophene) [6, 23] or polythiophene [7] and bisthienyl-based oligomers covalently attached to electrodes via a benzene spacer [7, 24]. Indeed, conducting polymers and oligomers can reversibly switch from a reduced insulating state to an oxidized conducting state depending on their doping level [25], leading to a change in their dielectric constant [26, 27]. The effect on the LSPR depends on the size and the shape of the NPs, and on the nature and the thickness of the conducting polymer film deposited on them. The LSPR can be either shifted or damped, depending on the system investigated.

In this paper, two main goals will be addressed. Firstly, we describe a simple new method for obtaining gold NPs by electrochemistry and compare these AuNP substrates with those obtained by *e*-beam lithography. In particular, their localized surface plasmon resonance (LSPR) has been investigated. Secondly, these plasmonic substrates have been used to generate active plasmonic devices by covering the AuNPs with an ultrathin organic film of bisthienylbenzene (BTB). The effect of the conductance switch of this electro-active organic layer on the properties of AuNPs is reported.

## 2. Experimental

### 2.1. Chemical reagents

All chemical products were purchased from Sigma-Aldrich and used without further purification. Indium tin oxide (ITO)-coated glass plates with a resistance of 30–50 $\Omega$/square were purchased from Solems.

### 2.2. Materials

A CHI 440A electrochemical workstation (CH instruments) was employed in all electrochemical experiments, which were carried out with a conventional one-compartment three-electrode cell. A Zeiss Supra 40 scanning electron microscope was used to evaluate the shape and size of AuNPs. The LSPR of AuNPs was recorded using an Ocean Optics HR4000 UV-visible spectrophotometer.

### 2.3. Electron beam lithography

AuNPs arrays were obtained by electron beam lithography (EBL) performed with a Zeiss Supra 40 scanning electronic microscope (SEM) equipped with a lithographic system (NPGS software). In a first step, a 180 nm thick polymethyl-

methacrylate (PMMA in chlorobenzene, from AllResist) layer was spin coated onto freshly cleaned ITO (with acetone, ethanol and propan-2-ol) and baked at 180 °C to evaporate the solvent. Then, the substrates were exposed to the electron beam, with a typical dose of 370 $\mu$C cm$^{-2}$. After exposure, chemical development was performed using methylisobutylketone: propan-2-ol (1:3) and then pure propan-2-ol was used to stop the development. Then, a 50 nm thick layer of gold was deposited by an ultravacuum evaporation process (Plassys MEB550S) with an evaporation rate of approximately 0.05 nm s$^{-1}$. Finally, a lift-off process was performed using acetone in order to remove the remaining PMMA layer together with the gold layer on top whereas, in the areas exposed to the electron beam, the AuNPs resting directly on the ITO substrate remained. The total size of the gratings produced by EBL was limited to 100 $\mu$m squares.

### 2.4. Electrodeposition of gold NPs

ITO electrodes were cleaned by sonication for 20 min in dilute alkaline Extran®solution (Merck), then carefully rinsed with distilled water and then ethanol; they were stored in ultrapure milli-Q water (18.2 M$\Omega$ cm$^{-1}$) until required for AuNP electrodeposition. Electrodeposition experiments were carried out by the chronoamperometry technique in a stirred aqueous solution of $2.10^{-3}$ M KAuCl$_4$ and 0.25 M Na$_2$CO$_3$. The reference was a saturated calomel electrode (SCE) and the counter-electrode was a stainless steel grid. The solution was maintained under argon atmosphere during the whole experiment. AuNPs were deposited on ITO electrodes at a constant potential and a controlled total charge current density.

### 2.5. BTB grafting

1-(2-Bisthienyl)-4-aminobenzene (BTAB) was synthesized as previously described [28]. Grafting onto substrates was performed using *in situ* diazonium salt formation: under argon 30 eq. of *tert*-butyl nitrite were added to a 0.5 mM solution of BTAB in acetonitrile containing 0.1 M of tetra-n-butylammonium tetrafluoroborate (TBABF$_4$). BTB was grafted by multi-scan cyclic voltammetry (CV) (15 successive cycles) in the cathodic range (between 0.3 and −0.5 V/SCE) at a scan rate of 100 mV s$^{-1}$. By this means, films less than 15 nm thick are generated. A full description of the measurement of the thickness of BTB on gold gratings generated by *e*-beam can be found in a previous publication [7].

### 2.6. Localized surface plasmon resonance (LSPR) measurements under electrochemical control

To make LSPR measurements under electrochemical control, a home-made planar three-electrode cell with a stainless steel grid counter-electrode and a silver (Ag/AgCl) pseudo-reference electrode was used. The AuNP array-modified working electrode was placed horizontally on the bottom. The cell was then filled with the electrolyte solution. Absorption measurements were carried out with an Ocean Optics HR 4000 UV–visible spectrophotometer coupled with a fiber-optic
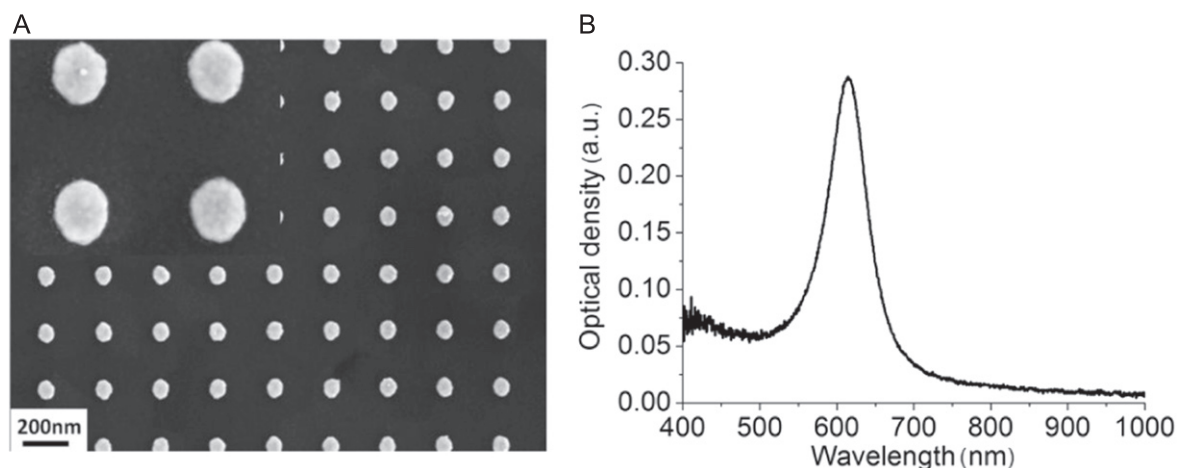
**Figure 1.** (A) SEM image of an AuNP array obtained onto ITO using *e*-beam lithography method (oblate particles, 80 nm in diameter, 50 nm high and 250 nm gratings), (B) optical extinction spectrum corresponding to this arrays.

system which made it possible to analyze an area of $80\,\mu\text{m} \times 80\,\mu\text{m}$. Modulation of LSPR signals was checked by switching the applied potential between a cathodic and an anodic value, either by chronoamperometry or by CV.

# 3. Results and discussion

## 3.1. AuNP arrays obtained by e-beam lithography

A classical route to AuNP substrates consists in using *e*-beam lithography. This method relies on the formation of a nano-hole-based template in a resin, drawn by the electron beam of a scanning electron microscope (SEM), followed by evaporating gold into the holes. After a lift-off step allowing to remove the resin, an AuNP array appears on the substrate. The process is explained in more detail in the experimental part of this paper.

Figure 1(A) shows the SEM image of a typical AuNP array obtained by this technique and figure 1(B) depicts the corresponding spectrum. The extinction band is attributed to the localized surface plasmon resonance (LSPR) of the AuNPs. The peak is very sharp, with its full-width at half-maximum (FWHM) around 70 nm, which indicates the homogeneity in size of the AuNPs.

The advantage of this technique is not only the possibility of obtaining very perfect AuNP arrays (every NP with the same size, a controlled distance between them, etc…), but also that of modulating the shape and size of the NPs, as well as the distance between them, at will. Nevertheless, this method is a multi-step process which requires not only a long time but also expensive apparatus (electron microscope and metal evaporation apparatus). Moreover, no large-area plasmonic substrates can be obtained by this technique (AuNP arrays are typically around $100\,\mu\text{m}$ wide using *e*-beam lithography).

In this context, there is a strong need to develop low-cost methods to obtain large-area AuNP plasmonic substrates, with good LSPR characteristics.

## 3.2. AuNP substrates obtained by electrochemistry

We propose an alternative method to obtain AuNP substrates based on the electrochemical reduction of a gold Au (III) salt. Electrodeposition of AuNP is performed using a chronoamperometric method from an aqueous $KAuCl_4$ solution (2 mM) containing $Na_2CO_3$ (0.25 M) as supporting electrolyte. After the electrochemical process, the ITO electrodes are red or blue, depending on the experimental conditions used, which is clear evidence for the deposition of gold at the nanoscale.

The influence of the potential value applied for gold deposition on the size and dispersity of the AuNPs has been investigated. Indeed, chronoamperometry was performed at various potentials, the total charge density used during the reduction process being fixed at $20\,\text{mC cm}^{-2}$. SEM images (figure 2) show that the size of the AuNPs decreases and their density increases when the electrodeposition potential becomes more negative. This is confirmed by the NP diameter distribution histograms constructed from these SEM images. Indeed, the average size of the AuNPs decreases from 150 nm to 90 nm when the reduction potential decreases from $-0.6$ V to $-1.0$ V/SCE. Similar analysis performed on various areas of the sample show no significant variation in the size of the AuNPs, which indicates that their deposition is quite uniform over the $2\,\text{cm}^2$ area of the ITO electrode.

Figure 3 shows the optical extinction spectra of the five AuNP substrates corresponding to the SEM images of figure 2, i.e. obtained at different reduction potentials (between $-0.6$ and $-1.0$ V/SCE) in fixing the total charge density at $20\,\text{mC cm}^{-2}$. For all samples, the strong absorption in the visible range can be attributed to the LSPR of AuNPs. Spectra taken in various areas of the sample do not show significant variation of the LSPR, confirming that AuNPs are uniformly deposited on the ITO electrode. The LSPR maximum wavelength is blue-shifted from 680 nm to 580 nm when the applied potential goes from $-0.6$ to $-1$ V/SCE, which is consistent with the formation of smaller AuNPs when it becomes more negative. Moreover, the full width at half maximum (FWHM) of the LSPR decreases from 200 to
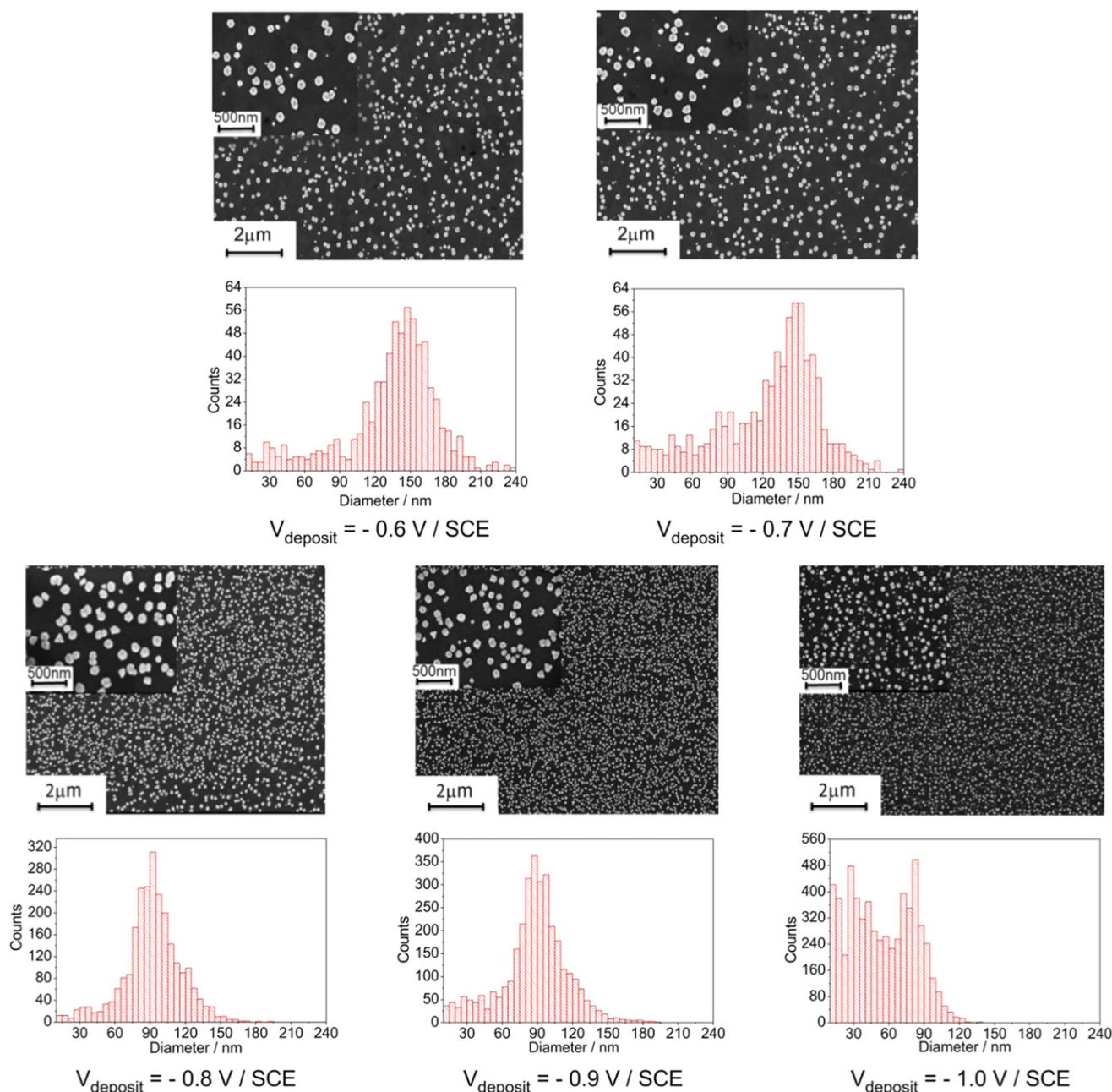
**Figure 2.** SEM images of AuNPs electrodeposited onto ITO at various reduction potentials ($-0.6$ to $-1.0$ V/SCE and fixed total charge density ($Q = 20$ mC cm$^{-2}$), and corresponding AuNP diameter distribution histograms.

80 nm on going from $-0.6$ to $-1$ V/SCE, showing an improvement in the optical response of the substrates. In particular, the sharpness of the LSPR signals observed for reduction potentials between $-0.8$ and $-1$ V/SCE is characteristic of plasmonic substrates with high quality factor, the FWHM being comparable to that of substrates obtained by *e*-beam lithography.

In these experiments, it appears that the potential used to reduce the gold salt has a marked influence on AuNP nucleation. Indeed, the higher the negative potential, the easier nucleation will be, leading to an increase in the number of nuclei and in the overall NP density. As the total charge density used during electroreduction was kept constant for each

deposition, a high density manifests itself in the formation of smaller NPs (at high negative potentials) while a low density leads to larger NPs (at low negative potentials). A more detailed explanation concerning the processes involved during the electrosynthesis of AuNPs has been recently published [24].

### 3.3. Electroactive plasmonic devices

#### 3.3.1. BTB electrografting onto AuNP electrodes.
These two kinds of AuNP substrates have been compared for use as plasmonic electrodes in electroactive plasmonic devices.

An ultrathin organic film of oligoBTB was deposited on each kind of electrode by electroreduction of the
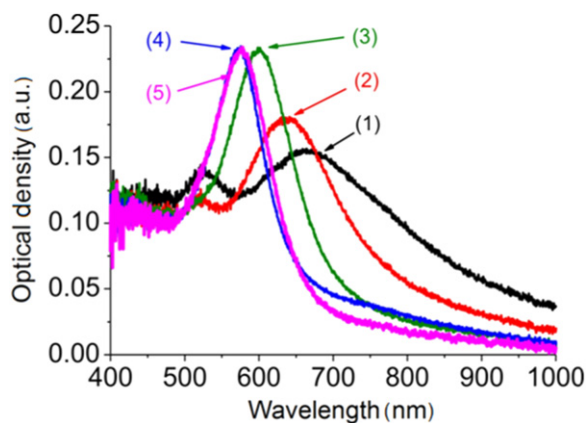
**Figure 3.** Optical extinction spectra of AuNPs on ITO electrodes obtained at various reduction potentials ($-0.6$ V (curve 1), $-0.7$ V (curve 2), $-0.8$ V (curve 3), $-0.9$ V (curve 4) and $-1$ V/SCE (curve 5)) and with a total charge density, $Q = 20$ mC cm$^{-2}$.
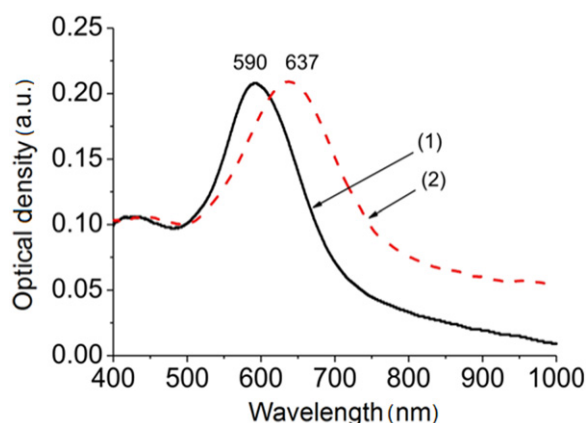


**Figure 4.** Optical extinction spectra of an AuNP electrode obtained by electrodeposition ($-0.8$ V/SCE and 20 mC cm$^2$), before (curve 1) and after (curve 2) BTB deposition.

corresponding diazonium salt [28]. The resulting covalently bonded layer is less than 15 nm thick [7]. Such a molecular film is known to undergo a reversible conductance change with variation of the voltage [28, 29], switching between a totally blocking reduced state and a conducting oxidized state at close to 0.6 V/SCE. Such a conductance switch can induce a change in the dielectric constant of the BTB layer and affect the LSPR signal.

After BTB had been grafted onto the AuNP substrates, a red-shift of the LSPR was observed (figure 4), whatever the process used to perform AuNP substrates. This red-shift of 40–70 nm is attributed to the modification of the dielectric environment [30–32] induced by the deposition of the thin film. Such a red-shift is commonly observed when the dielectric constant of the medium surrounding the NPs increases [7, 30–32].

*3.3.2. Electrochemical polarization of BTB|AuNP|ITO electrodes.* The effect of the BTB conductance switch on the LSPR of AuNPs was investigated by varying the

polarization of the BTB|AuNP electrodes. Ferrocene (Fc) was added to the electrolyte solution in order to ensure the stability of the BTB layer, since BTB is oxidized to reactive radical-cations. Indeed, under these conditions, BTB acts as a molecular bridge to oxidize Fc in solution and, thus, the accumulation of charges in the BTB film and solid-state coupling between reactive BTB radical cations, leading to film degradation, are avoided.

Figures 5(A) and (B) display the optical extinction spectra of BTB|AuNP devices obtained by *e*-beam lithography and electrodeposition, respectively, during the electrochemical switch from the reduced state to the oxidized state of BTB. Similar effects are observed whatever the BTB|AuNP electrode used. Indeed, a broadening accompanied by a decrease in the intensity of the LSPR band is observed, clearly showing modulation of the LSPR by the switching of the thin layer of BTB. Nevertheless, no shift of the LSPR band is observed. These dampings are large compared to previously reported equivalent systems. Indeed, while marked dampings are observed when thick layers (for example, a layer of a conducting polymer such as a PANI film) are deposited on AuNPs [5], the effects are generally smaller for NP systems using ultrathin films or molecular monolayers [22]. The quite large damping observed in our case can be attributed to the covalent bonds between the BTB and the AuNPs [7].

Such observations can be qualitatively explained by the Drude free-electron model [33–35], in which the dielectric function of a conductive material is complex ($\varepsilon = \varepsilon_{\mathrm{Re}} + i\varepsilon_{\mathrm{Im}}$) while the dielectric function of an insulating material is described only by a real value. In our case, the observed damping of the LSPR band, when the BTB layer shifts from its reduced state to its oxidized state, indicates that the imaginary part of the dielectric constant ($\varepsilon_{\mathrm{Im}}$) of the BTB increases sharply, which is in agreement with a switch of the BTB film between an insulating and a conducting state [7, 26, 27]. This damping can be attributed to charge transfer between plasmon-generated hot electrons and the BTB film in its conducting state, which acts as an efficient acceptor, the LSPR lifetime being decreased by the presence of an additional decay channel [36]. On the other hand, the absence of LSPR band shift when the BTB film is switched indicates that the real part of the dielectric constant ($\varepsilon_{\mathrm{Re}}$) of the film does not change significantly [7, 26, 27].

A more detailed study can be performed by scanning the potential by CV. Figure 6 shows how the intensity at the LSPR maximum and its FWHM depend on the potential applied during the CV, in the case of a BTB|AuNP electrode obtained by electrodeposition. In the forward scan, as long as the BTB film remains in its blocking state, i.e. when the potential is below 0.6 V/SCE, no or very little LSPR modulation occurs. However, when charges are injected into the BTB film, leading to its conductive state, the LSPR signal is progressively damped. Note also that the initial LSPR signal was restored upon polarization of the film at 0 V.
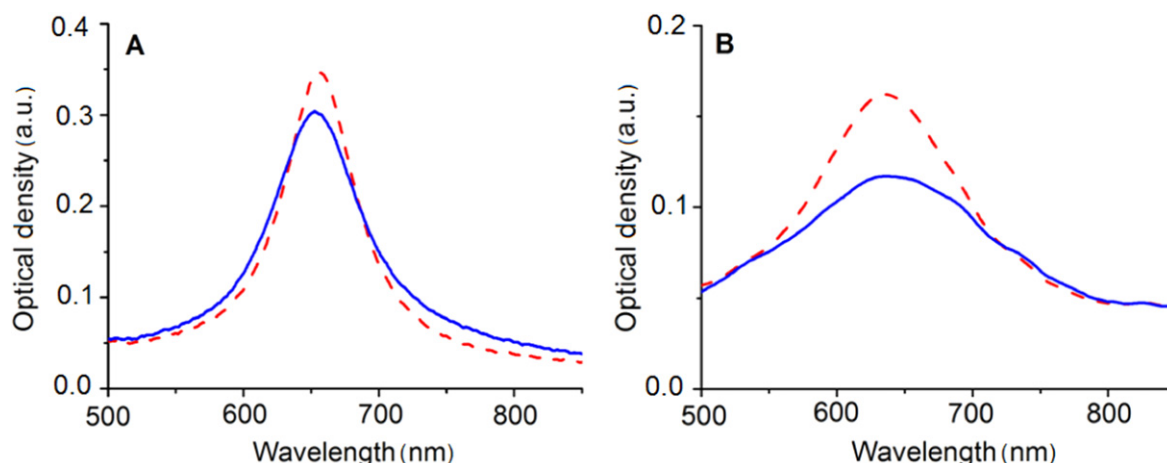
**Figure 5.** Optical extinction spectra AuNP electrodes obtained by (A) *e*-beam lithography and (B) electrodeposition, and overcoated with an 8–12 nm BTB film in its reduced state (0.2 V/SCE, red dashed line) and in its oxidized state (0.9 V/SCE, blue full line).
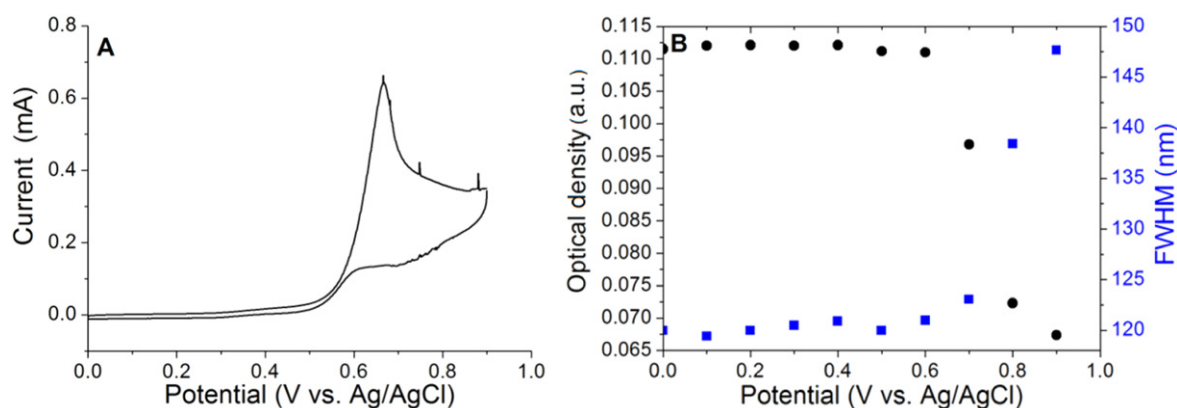


**Figure 6.** (A) CV of Fc (1 mM) in 1 M $LiClO_4$ solution in acetonitrile on a BTB/AuNP electrode obtained by gold electroreduction (scan rate: 100 mV s$^{-1}$) and (B) variation of the LSPR band intensity maximum and FWHM of this band during one CV scan.

## 4. Conclusions

In this work we have compared electroactive plasmonic devices using AuNP|ITO electrodes obtained in two different ways: *e*-beam lithography and electroreduction of an Au III salt by chronoamperometry. The first method (*e*-beam lithography) leads to very well ordered AuNP arrays. Nevertheless, this technique is a multi-step process with requires not only a long time but also expensive apparatus (electron microscope and metal evaporation apparatus). Moreover, it allows to generate only very small AuNP arrays, typically around 100 $\mu$m wide. On the contrary, the second method (electroreduction of a gold salt) is a low-cost technique allowing the formation of large-area AuNP plasmonic substrates. Despite the lack of organization of the NPs, the AuNP substrates produced by this method have an optical response close to that of the samples fabricated by *e*-beam deposition. Moreover, AuNP substrates are obtained by electrochemistry on electrodes of several square centimeters in area in less than 100 s in a one-step template-free process.

In a second step, these plasmonic AuNP electrodes were covered with an ultrathin organic film of BTB which displays a reversible voltage-dependent switch between a conducting and an insulating state. The effect of this conductance switch on the plasmonic properties of the AuNPs was studied, and the results were the same whatever the method of preparation of the AuNP substrate. When the film is switched from its insulating state to its conducting state, a marked damping of the LSPR band, with a large intensity decrease and a strong FWHM increase, is observed. These observations indicate that the LSPR lifetime of AuNPs is smaller when BTB is in its conducting state. These changes are probably due to charge transfer between plasmon-generated hot electrons and the conducting BTB, which acts as an efficient electron acceptor. It is remarkable that this large LSPR modulation is obtained with a film which is less than 12 nm thick. These results are important to academic investigations of nanoscale materials. In view of the increasing demand for ultimate miniaturization of electronic and photonic systems, applications of active plasmonic devices as sensors or routers can be foreseen.

Adv. Nat. Sci.: Nanosci. Nanotechnol. **7** (2016) 015005

V-Q Nguyen *et al*

the University of Science and Technology of Hanoi (Vietnam).

# References

[1] Gole A, Orendorff C J and Murphy C J 2004 *Langmuir* **20** 7117

[2] Brust M, Bethell D, Kiely C J and Schiffrin D J 1998 *Langmuir* **14** 5425

[3] Leroux Y R, Lacroix J C, Chane-Ching K I, Fave C, Félidj N, Lévi G, Aubard J, Krenn J R and Hohenau A 2005 *J. Am. Chem. Soc.* **127** 16022

[4] Leroux Y, Lacroix J C, Fave C, Trippé G, Félidj N, Aubard J, Hohenau A and Krenn J R 2008 *ACS Nano* **2** 728

[5] Leroux Y, Lacroix J C, Fave C, Stockhausen V, Félidj N, Grand J, Hohenau A and Krenn J R 2009 *Nano Lett.* **9** 2144

[6] Stockhausen V, Martin P, Ghilane J, Leroux Y, Randriamahazaka H, Grand J, Félidj N and Lacroix J C 2010 *J. Am. Chem. Soc.* **132** 10224

[7] Schaming D, Nguyen V Q, Martin P and Lacroix J C 2014 *J. Phys. Chem.* C **118** 25158

[8] Hulteen J C and Van Duyne R P 1995 *J. Vac. Sci. Technol.* A **13** 1553

[9] Ye X and Qi L 2011 *Nano Today* **6** 608

[10] Hulteen J C, Treichel D A, Smith M T, Duval M L, Jensen T R and Van Duyne R P 1999 *J. Phys. Chem.* B **103** 3854

[11] Sakai N, Fujiwara Y, Arai M, Yu K and Tatsuma T 2009 *J. Electroanal. Chem.* **628** 7

[12] Fernàndez-Blanco C, Colina A, Heras A, Ruiz V and Lopez-Palacios J 2012 *Electrochem. Commun.* **18** 8

[13] Karg M, Pastoriza-Santos I, Pérez-Juste J, Hellweg T and Liz-Marzan L M 2007 *Small* **3** 1222

[14] Gehan H, Mangeney C, Aubard J, Lévi G, Hohenau A, Krenn J R, Lacaze E and Félidj N 2011 *J. Phys. Chem. Lett.* **2** 926

[15] Abdul-Kader K *et al* 2013 *Nanoscale* **5** 5288

[16] Pita M, Krämer M, Zhou J, Poghossian A, Schöning M J, Fernandez V M and Katz E 2008 *ACS Nano* **2** 2160

[17] Sidhaye D S, Kashyap S, Sastry M, Hotha S and Prasad B L V 2005 *Langmuir* **21** 7979

[18] Hira T, Homma T, Uchiyama T, Kuwamura K and Saiki T 2013 *Appl. Phys. Lett.* **103** 241101

[19] Khatua S, Chang W S, Swanglap P, Olson J and Link S 2011 *Nano Lett.* **11** 3797

[20] Wang Z and Chumanov G 2003 *Adv. Mater.* **15** 1285

[21] Leroux Y, Eang E, Fave C, Trippé G and Lacroix J C 2007 *Electrochem. Commun.* **9** 1258

[22] Zheng Y B, Yang Y W, Jensen L, Fang L, Juluri B K, Flood A H, Weiss P S, Stoddart J F and Huang T J 2009 *Nano Lett.* **9** 819

[23] Baba A, Tada K, Janmanee R, Sriwichai S, Shinbo K, Kato K, Kaneko F and Phanichphant S 2012 *Adv. Funct. Mater.* **22** 4383

[24] Nguyen V Q, Schaming D, Martin P and Lacroix J C 2015 *Electrochim. Acta* **179** 282

[25] Inzelt G 2008 *Conducting Polymers—A New Area in Electrochemistry* ed F Scholtz (Berlin: Springer)

[26] Baba A, Lübben J, Tamada K and Knoll W 2003 *Langmuir* **19** 9058

[27] Baba A, Tian S, Stefani F, Xia C, Wang Z, Advincula R C, Johannsmann D and Knoll W 2004 *J. Electroanal. Chem.* **562** 95

[28] Fave C, Leroux Y, Trippé G, Randriamahazaka H, Noel V and Lacroix J C 2007 *J. Am. Chem. Soc.* **129** 1890

[29] Stockhausen V, Ghilane J, Martin P, Trippe-Allard G, Randriamahazaka H and Lacroix J C 2009 *J. Am. Chem. Soc.* **131** 14920

[30] Jensen T R, Duval M L, Kelly K L, Lazarides A A, Schatz G C and Van Duyne R P 1999 *J. Phys. Chem.* B **103** 9846

[31] Kelly K L, Coronado E, Zhao L L and Schatz G C 2003 *J. Phys. Chem.* B **107** 668

[32] Miller M M and Lazarides A A 2005 *J. Phys. Chem.* B **109** 21556

[33] Kohlman R S, Joo J, Min Y G, MacDiarmid A G and Epstein A J 1996 *Phys. Rev. Lett.* **77** 2766

[34] Prigodin V N and Epstein A J 2002 *Synthetic Met.* **125** 43

[35] Tzamalis G, Zaidi N A, Homes C C and Monkman A P 2002 *Phys. Rev.* B **66** 085202

[36] Hoggard A, Wang L Y, Ma L, Fang Y, You G, Olson J, Liu Z, Chang W S, Ajayan P M and Link S 2013 *ACS Nano* **7** 11209